

# UC San Diego

## UC San Diego Previously Published Works

### Title

APOL1 Kidney-Risk Variants Induce Mitochondrial Fission

### Permalink

<https://escholarship.org/uc/item/9994h3b7>

### Journal

Kidney International Reports, 5(6)

### ISSN

2468-0249

### Authors

Ma, Lijun  
Ainsworth, Hannah C  
Snipes, James A  
et al.

### Publication Date

2020-06-01

### DOI

10.1016/j.ekir.2020.03.020

Peer reviewed

# APOL1 Kidney-Risk Variants Induce Mitochondrial Fission



Lijun Ma<sup>1</sup>, Hannah C. Ainsworth<sup>2</sup>, James A. Snipes<sup>1</sup>, Mariana Murea<sup>1</sup>, Young A Choi<sup>1</sup>, Carl D. Langefeld<sup>2</sup>, John S. Parks<sup>3</sup>, Manish S. Bharadwaj<sup>4</sup>, Jeff W. Chou<sup>2</sup>, Ashok K. Hemal<sup>5</sup>, Snezana Petrovic<sup>4</sup>, Ann L. Craddock<sup>6</sup>, Dongmei Cheng<sup>3</sup>, Gregory A. Hawkins<sup>6</sup>, Lance D. Miller<sup>6</sup>, Pamela J. Hicks<sup>7</sup>, Moin A. Saleem<sup>8</sup>, Jasmin Divers<sup>2</sup>, Anthony J. A. Molina<sup>4</sup> and Barry I. Freedman<sup>1</sup>

<sup>1</sup>Department of Internal Medicine, Section on Nephrology, Wake Forest School of Medicine, Winston-Salem, North Carolina, USA; <sup>2</sup>Division of Public Health Sciences, Department of Biostatistics and Data Science, Wake Forest School of Medicine, Winston-Salem, North Carolina, USA; <sup>3</sup>Department of Internal Medicine, Section on Molecular Medicine, Wake Forest School of Medicine, Winston-Salem, North Carolina, USA; <sup>4</sup>Department of Internal Medicine, Section on Gerontology and Geriatric Medicine, Wake Forest School of Medicine, Winston-Salem, North Carolina, USA; <sup>5</sup>Department of Urology, Wake Forest School of Medicine, Winston-Salem, North Carolina, USA; <sup>6</sup>Department of Cancer Biology, Wake Forest School of Medicine, Winston-Salem, North Carolina, USA; <sup>7</sup>Department of Biochemistry, Wake Forest School of Medicine, Winston-Salem, North Carolina, USA; and <sup>8</sup>Children's Renal Unit, Bristol Royal Hospital for Children, University of Bristol, Bristol, United Kingdom

**Introduction:** *APOL1* G1 and G2 nephropathy-risk variants cause mitochondrial dysfunction and contribute to kidney disease. Analyses were performed to determine the genetic regulation of *APOL1* and elucidate potential mechanisms in *APOL1*-nephropathy.

**Methods:** A global gene expression analysis was performed in human primary renal tubule cell lines derived from 50 African American individuals. Follow-up gene knock out, cell-based rescue, and microscopy experiments were performed.

**Results:** *APOL1* genotypes did not alter *APOL1* expression levels in the global gene expression analysis. Expression quantitative trait locus (eQTL) analysis in polyinosinic-polycytidylic acid (poly IC)-stimulated renal tubule cells revealed that single nucleotide polymorphism (SNP) rs513349 adjacent to *BAK1* was a *trans* eQTL for *APOL1* and a *cis* eQTL for *BAK1*; *APOL1* and *BAK1* were co-expressed in cells. *BAK1* knockout in a human podocyte cell line resulted in diminished *APOL1* protein, supporting a pivotal effect for *BAK1* on *APOL1* expression. Because *BAK1* is involved in mitochondrial dynamics, mitochondrial morphology was examined in primary renal tubule cells and HEK293 Tet-on cells of various *APOL1* genotypes. Mitochondria in *APOL1* wild-type (G0G0) tubule cells maintained elongated morphology when stimulated by low-dose poly IC, whereas those with G1G1, G2G2, and G1G2 genotypes appeared to fragment. HEK293 Tet-on cells overexpressing *APOL1* G0, G1, and G2 were created; G0 cells appeared to promote mitochondrial fusion, whereas G1 and G2 induced mitochondrial fission. The mitochondrial dynamic regulator Mdivi-1 significantly preserved cell viability and mitochondrial cristae structure and reversed mitochondrial fission induced by overexpression of G1 and G2.

**Conclusion:** Results suggest the mitochondrial fusion/fission pathway may be a therapeutic target in *APOL1*-nephropathy.

*Kidney Int Rep* (2020) 5, 891–904; <https://doi.org/10.1016/j.ekir.2020.03.020>

KEYWORDS: African Americans; *APOL1*; chronic kidney disease; FSGS; mitochondria

© 2020 International Society of Nephrology. Published by Elsevier Inc. This is an open access article under the CC BY-NC-ND license (<http://creativecommons.org/licenses/by-nc-nd/4.0/>).

**Correspondence:** Lijun Ma, Department of Internal Medicine, Section on Nephrology, Wake Forest School of Medicine, Medical Center Boulevard, Winston-Salem, North Carolina 27157, USA. E-mail: [lima@wakehealth.edu](mailto:lima@wakehealth.edu); or Barry I. Freedman, Department of Internal Medicine, Section on Nephrology, Wake Forest School of Medicine, Medical Center Boulevard, Winston-Salem, North Carolina 27157, USA. E-mail: [bfreedma@wakehealth.edu](mailto:bfreedma@wakehealth.edu)

Received 28 December 2019; revised 28 February 2020; accepted 16 March 2020; published online 30 March 2020

Since discovery of the apolipoprotein L1 gene (*APOL1*) association with chronic kidney disease in populations with recent African ancestry,<sup>1,2</sup> efforts have been undertaken to elucidate mechanisms whereby the common G1 (2 variants, S342G and I384M, in nearly perfect linkage disequilibrium) and G2 (deletion of amino acids N388 and Y389) kidney-risk variants (KRVs) cause nephropathy.<sup>3–5</sup> Endogenous and locally acting (not circulating) *APOL1* protein appears to cause nephropathy based on data from kidney

transplantation, cell biology, and animal models.<sup>6–15</sup> Ma *et al.*<sup>16</sup> and Granado *et al.*<sup>17</sup> independently reported that reduced mitochondrial function caused by *APOL1* G1 and G2 KRVs contribute to chronic kidney disease. Shah *et al.*<sup>18</sup> reported that *APOL1* KRVs induce cell death via mitochondrial translocation and opening of the inner mitochondrial membrane permeability transition pore. *APOL1* is widely present in mitochondria<sup>17</sup> and adverse effects could extend beyond permeability changes in the inner membrane. Mitochondrial dysfunction is also known to cause non-*APOL1*-mediated kidney diseases.<sup>19</sup>

Most individuals with 2 *APOL1* KRVs do not develop nephropathy; a modifier is required.<sup>20</sup> Proven modifiers include HIV-induced alterations in the immune response and administration of interferons.<sup>21</sup> In these settings, *APOL1* expression levels are increased via the toll-like receptor 3 (TLR3)-dependent pathway. This report assessed pathways potentially leading to *APOL1*-nephropathy and further implicated compromised mitochondrial function based on the results of a global gene expression analysis in primary human renal proximal tubule cells (PTCs) from African American individuals. Cells were exposed to an immune system activator (poly IC) to provide a stressor mimicking viral infection. Expression quantitative trait locus (eQTL) analysis and fluorescence microscopy were performed, with subsequent gene knockout to verify effects of an *APOL1* upstream regulator identified in an eQTL analysis. To determine whether increased *APOL1* G1 and G2 KRV expression directly contributed to mitochondrial effects, HEK293 Tet-on cell lines overexpressing *APOL1* G0 (wild-type), G1, and G2 KRVs were used to assess the pathways affecting mitochondrial function by immunoblotting and fluorescence microscopy; these cells have minimal or no TLR3 expression. Finally, mitochondrial rescue was performed by blocking implicated pathways to confirm mechanisms underlying mitochondrial dysfunction and cell injury.

## METHODS

Full methods are provided in the [Supplementary Materials](#). In brief, total RNAs from human renal PTCs obtained from 50 African American individuals with an estimated glomerular filtration rate >60 ml/min per 1.73 m<sup>2</sup> undergoing surgical nephrectomy were isolated to perform global gene expression using Affymetrix HTA 2.0 arrays. DNA was isolated from peripheral blood, and Illumina (San Diego, CA) Multi-Ethnic Genotyping Arrays were used to genotype SNPs throughout the genome. The study was approved by the Wake Forest School of Medicine Institutional

Review Board and participants provided written informed consent. Gene knockout was performed using the corresponding CRISPR/Cas9 plasmids and transfection reagents provided by Santa Cruz Biotechnology (Dallas, TX). HEK293 Tet-on *APOL1* G0, G1, G2, and empty vector (EV) cells were established as previously reported.<sup>22</sup> Reverse transcriptase-polymerase chain reaction (RT-PCR), immunoblotting, and fluorescence were performed using established protocols.<sup>10,23</sup> Mitochondrial length was assessed using Fiji software, integrated with a plug-in macro toolset Mitochondrial Network Analysis.<sup>24</sup> Cell viability was measured using a Cytotox 96 lactate dehydrogenase viability assay kit (Promega, Madison, WI) per manufacturer instructions.

## RESULTS

### Pathway Analysis in Primary Renal PTC Lines With and Without Stimulation by Poly IC

Primary renal PTCs were treated with 2.5 µg/ml poly IC for 16 hours to stimulate the innate immune response while maintaining viability, conditions that upregulated *APOL1* expression 8- to 15-fold and *TLR3* expression 15- to 20-fold, with minimal changes in cell viability (data not shown). Global gene expression profiles in the 50 primary renal PTC lines from African American individuals were computed using CytoScape-based BiNGO. Among 1212 upregulated genes, 9 of the top 20 associated pathways related to immune response as anticipated with poly IC exposure. In 1060 downregulated genes, mitochondrial and related pathways were among the top 20 associated pathways ([Supplementary Table S1](#)). Index pathways were verified by Ingenuity Pathway Analysis (QIAGEN, Hilden, Germany) ([Supplementary Tables S2A and S2B](#)).

### *APOL1* eQTL Global Gene Expression Analyses and Genome-Wide Association Study of *APOL1* mRNA Expression

To assess whether *APOL1* KRVs in an additive (0 vs. 1 vs. 2) or recessive genetic model (0/1 vs. 2) affected *cis* and *trans* gene expression levels, global gene expression profiles in the African American primary renal PTC lines were estimated by Affymetrix (Santa Clara, CA) HTA 2.0 arrays. *APOL1* KRVs did not significantly affect baseline or post-poly IC *APOL1* expression levels, or expression of *APOL2*, *APOL3*, *APOL4*, *APOL5*, *APOL6*, or *MYH9* (non-muscle myosin heavy chain 9 gene) (data not shown). Considering multiple testing, *APOL1* KRVs did not significantly alter global *trans* gene expression (data not shown).

To determine whether *APOL1* expression was affected by *cis*- or *trans*-regulating loci, a genome-wide association study with *APOL1* expression level was performed. To maximize information from the small

sample, a minor allele frequency criterion  $\geq 0.05$  was required, yielding 731,553 SNPs for analyses. Baseline, post-poly IC, and the difference between post-poly IC and baseline *APOL1* mRNA levels were analyzed (Figure 1). The top associations with baseline and post-poly IC *APOL1* were rs6559850 at 9q21 ( $P = 7.4 \times 10^{-7}$ ) and rs513349 at 6p21 ( $P = 2.4 \times 10^{-7}$ ), respectively; these did not reach the genome-wide association study significance threshold (Table 1 and Figure 1). Both rs142546651 at 3q26 and rs148695969 at 13q21 reached genome-wide association study significance for association with the difference in *APOL1* expression after poly IC, compared with baseline (Figure 1c). SNP rs148695969 resides in a gene desert and follow-up for *cis* eQTLs was not attempted.

SNP rs6559850 was not a significant *cis* eQTL for adjacent genes (data not shown). In contrast, rs513349 was an eQTL for the adjacent BCL2 Antagonist/Killer 1 gene (*BAK1*) ( $P = 0.003$ – $0.004$ ) (Figure 2), and was co-expressed with *APOL1* after poly IC ( $R = 0.7$ ;  $P < 0.0001$ ; Figure 3) independent of *APOL1* genotype ( $t = -1.08$ ,  $P = 0.29$ ). *BAK1* is a mitochondrial protein (Supplementary Figures S1 and S2) present in human renal tubule cells and podocytes (Supplementary Figure S3). At baseline (before poly IC), rs142546651 was a *cis* eQTL for the *SLIT* and *NTRK*-like family member 3 gene (*SLITRK3*). However, no association was found for *SLITRK3* and *APOL1* expression in primary renal PTCs at baseline, post-poly IC, or for the difference between post-poly IC and baseline. Hence, only the top *trans* eQTL rs513349 for *APOL1* was evaluated as a *cis* eQTL for the adjacent *BAK1* gene. This revealed that rs513349 could affect *APOL1* gene expression via *BAK1*, particularly after poly IC exposure.

### **APOL1 Is Regulated by BAK1 in Human Podocytes**

To verify results from the genome-wide search for eQTLs of *APOL1* where *BAK1* could be an upstream regulator of *APOL1* expression, the *BAK1* gene was knocked out in a human podocyte cell line using CRISPR/Cas9 technology. *APOL1* mRNA level was less responsive to poly IC treatment in *BAK1* knockout cells than in wild-type cells (Supplementary Figure S4). After *BAK1* knockout, *BAK1* protein was undetectable by immunoblotting and immunofluorescence (Supplementary Figures S5 and S6). *APOL1* protein level was markedly reduced after *BAK1* knock out (Supplementary Figures S5 and S6). Low-concentration poly IC (0.15  $\mu\text{g/ml}$ ) increased the expression level of *BAK1* and *APOL1* when *BAK1* was present. When *BAK1* was knocked out, the effect of poly IC on *APOL1* upregulation was significantly diminished, indicating

the level of *APOL1* expression was largely related to presence of *BAK1* (Supplementary Figures S5 and S6).

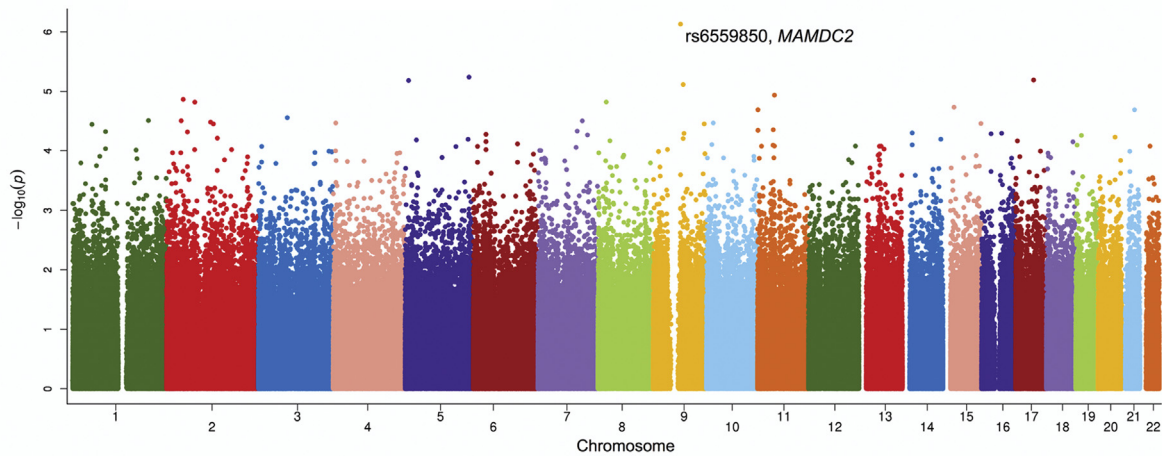
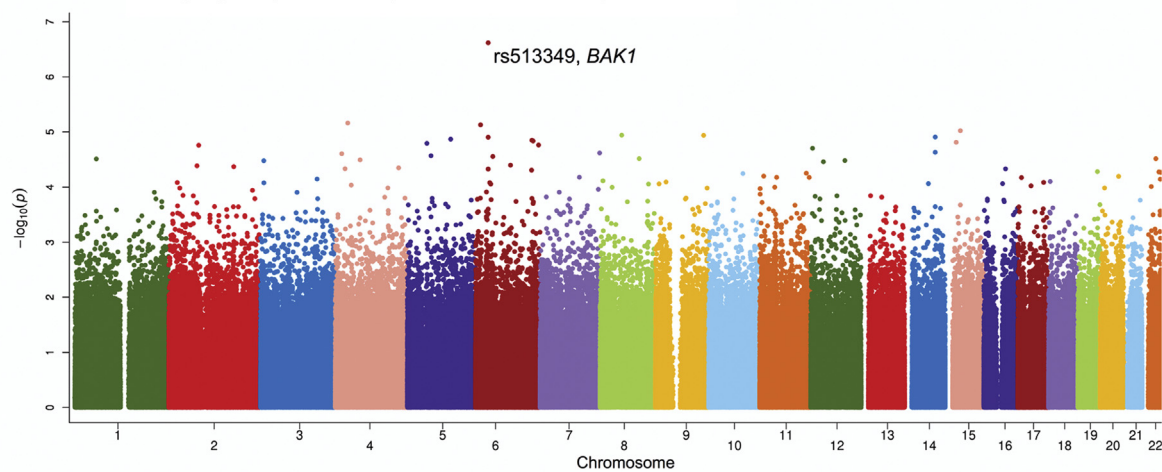
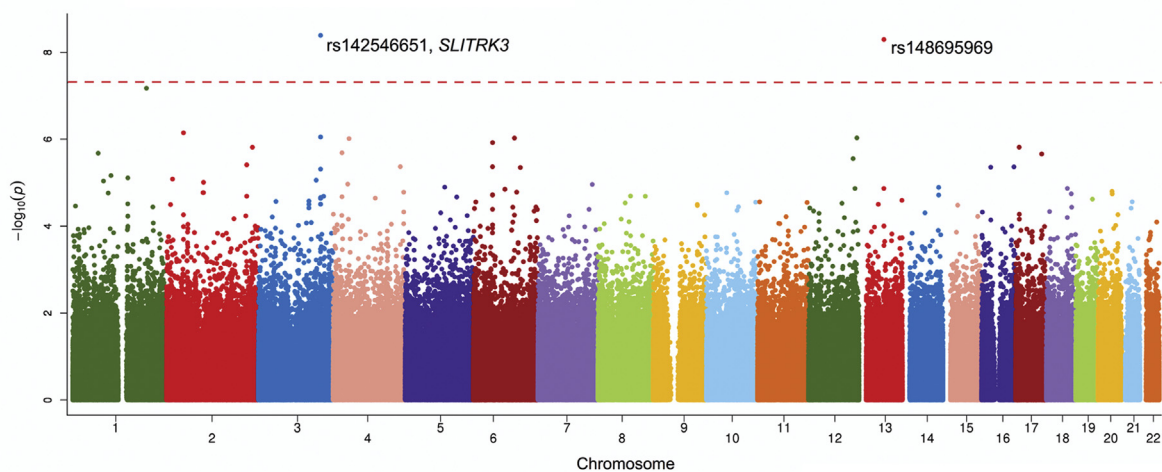
### **Poly IC Induces Mitochondrial Fragmentation in Primary Renal PTCs Homozygous for APOL1 G1 and G2**

*APOL1* KRVs modify mitochondrial function.<sup>16</sup> In addition, *APOL1* expression was affected by the mitochondrial protein *BAK1*, critical for mitochondrial dynamics.<sup>25</sup> Therefore, mitochondrial morphology was assessed in primary renal PTCs from 50 primary PTC lines from African American individuals. Two individuals homozygous for G0, 2 homozygous for G1, 2 with the compound G1/G2 risk genotype, and the single individual homozygous for G2 were chosen to estimate mitochondrial dynamics using confocal microscopy. Among the 2 individuals with each genotype, 1 woman and 1 man were selected. Individuals with 2 *APOL1* KRVs were similar in age to those without risk alleles ( $62.0 \pm 14.7$  vs.  $69.0 \pm 2.8$  years;  $P = 0.56$ ). Mitochondrial morphology was captured using MitoTracker Red (Figure 4a). Homozygous G0, G1, G2, and G1/G2 compound renal PTCs all exhibited elongated mitochondria before poly IC. However, cells with 2 copies of *APOL1* KRVs exhibited mitochondrial fragmentation after exposure to low-concentration poly IC (2.5  $\mu\text{g/ml}$  for 16 hours); mitochondrial morphology remained largely intact in renal PTCs from the individuals homozygous for G0 (Figure 4b–e).

### **APOL1 G1 and G2 Variants Induce Mitochondrial Fission in HEK293 Tet-On Cell Lines**

The observed mitochondrial fragmentation could relate to specific overexpression of *APOL1* G1 and G2 KRVs by poly IC or as a general effect of poly IC triggering the TLR3-mediated innate immune response. Hence, we assessed HEK293 Tet-on *APOL1* cell lines conditionally expressing G0, G1, and G2 variants, where the TLR3 pathway is absent.<sup>26</sup> Cells were assessed with and without exposure to low concentrations of doxycycline (Dox) to induce moderate *APOL1* expression. To clarify whether the observed fragmentation was typical G1- or G2-induced mitochondrial fission before moving into confocal imaging on HEK 293 Tet-on cells, immunoblotting was performed to determine the expression of mitochondrial fusion and fission proteins in HEK293 Tet-on *APOL1* (G0, G1, and G2) cell lines with and without Dox-induced *APOL1* overexpression. To mimic chronic exposure to *APOL1* protein, a lower Dox concentration ( $\sim 10$  ng/ml) and longer exposure time (24 hours) were used to induce *APOL1* expression. Regardless of *APOL1* G0, G1, or G2 genotypes, *APOL1* mRNA expression levels in HEK293 Tet-on cells were  $\sim 8$ -fold increased after exposure to Dox when



**a** Outcome: baseline *APOL1* mRNA expression**b** Outcome: after poly IC (stimulated) *APOL1* mRNA expression**c** Outcome: change\* in *APOL1* mRNA expression

**Figure 1.** Genome-wide association map (Manhattan Plot) showing relative *APOL1* mRNA expression in 50 primary renal proximal tubule cell lines from African American individuals without nephropathy. A total of 731,553 variants with minor allele frequencies  $>0.05$  were evaluated. X-axis refers to chromosomal single nucleotide polymorphism (SNP) location; y-axis represents negative log transformed *P* values for SNP association with *APOL1* expression. (a) SNPs associated with baseline *APOL1* expression; (b) SNPs associated with polyinosinic-polycytidylic acid (poly IC)–stimulated *APOL1* expression; (c) SNPs associated with the difference in *APOL1* expression (post–poly IC minus baseline). \*Change reflects difference in *APOL1* gene expression (after poly IC vs. baseline).

**Table 1.** Association between top SNPs with relative *APOL1* mRNA expression in primary renal PTC lines from African American individuals

SNP	Position	Condition	Allele (M/m)	Adjacent gene ID	Model	<i>P</i> value	Beta (SE)	mAF	MM ( <i>n</i> )	Mm ( <i>n</i> )	mm ( <i>n</i> )
rs6559850	9:72531390	Baseline	C/T	<i>MAMDC2</i>	Dom	$7.4 \times 10^{-7}$	1.03 (0.18)	0.17	35	13	2
rs513349	6:33541719	Poly IC	G/A	<i>BAK1</i>	Add	$2.4 \times 10^{-7}$	0.88 (0.15)	0.34	23	20	7
rs142546651	3:164915128	Change <sup>a</sup>	C/G	<i>SLITRK3</i>	Dom	$4.1 \times 10^{-9}$	1.37 (0.20)	0.07	44	5	1
rs148695969	13:65987966	Change <sup>a</sup>	T/G		Dom	$5.1 \times 10^{-9}$	1.48 (0.21)	0.05	45	5	0

Beta, estimate was determined by the effect of minor allele; M, major allele; m, minor allele; mAF, minor allele frequency; poly IC, in polyinosinic-polycytidylic acid; PTC, proximal tubule cell; SNP, single nucleotide polymorphism.

<sup>a</sup>Change: difference between poly IC vs. baseline.

SNP position based on human reference sequence (GRCh37). Genetic models Dom and Add refer to dominant and additive, respectively. *P* values adjusted for African ancestry proportion. Individuals had an estimated glomerular filtration rate >60 ml/min per 1.73 m<sup>2</sup> (*N* = 50).

compared with G0 cells without Dox (Supplementary Figure S7A). Comparable amounts of protein were obtained for the reference APOL1 G0 and the G1 and G2 variants (Supplementary Figure S7B). The mitochondrial fusion proteins mitochondrial dynamin like GTPase (OPA1), mitofusin-1 (MFN1), and mitofusin-2 (MFN2) and fission 1 protein (Fis1) did not display specific patterns related to *APOL1* genotype or Dox-induced *APOL1* overexpression. The mitochondrial fission dynamin-1-like protein (DRP1) levels were higher in Dox(+)-induced G1 and G2 cells, compared with Dox(-) G1 and G2 cells, respectively; DRP1 protein levels were lower in Dox(+)-induced G0 cells compared with Dox(-) G0 cells (Supplementary Figure S8). This suggested that G1 and G2 promoted mitochondrial fission. Because active DRP1 (phospho-DRP1 at Ser 616, p-DRP1) is recruited to the outer mitochondrial membrane and mediates mitochondrial fission,<sup>27,28</sup> and Mdivi-1 inhibits DRP1 by reducing p-DRP1(Ser616) on mitochondria,<sup>29</sup> p-DRP1(Ser616) was assessed by immunofluorescence on HEK293 Tet-on *APOL1* cells. G0 overexpression reduced p-DRP1(Ser616), whereas G1 and G2 overexpression increased p-DRP1(Ser616). The DRP-1 inhibitor Mdivi-1 markedly reduced the p-DRP1(Ser616) level in HEK293 Tet-on cells overexpressing G1 or G2 (Supplementary Figure S9). Hence, confocal microscopy was performed on HEK293 Tet-on cells using MitoTracker Red as a mitochondrial tracer (Figure 5a). HEK293 Tet-on EV and G0 cells exhibited elongated mitochondria before and after Dox induction; however, cells overexpressing G1 and G2 variants exhibited increased mitochondrial fragmentation after Dox induction (compared with baseline). To test the involvement of the DRP1-dependent mitochondrial fission pathway based on *APOL1*, the mitochondrial fission inhibitor Mdivi-1 was used to determine whether mitochondrial morphological patterns could be restored. Mdivi-1 prevented the mitochondrial fragmentation induced by KRV *APOL1* overexpression in HEK293 Tet-on cells. Mdivi-1 did not alter the mitochondrial morphology in HEK293 Tet-on EV and G0 cells after treatment with Dox (Figure 5b-e).

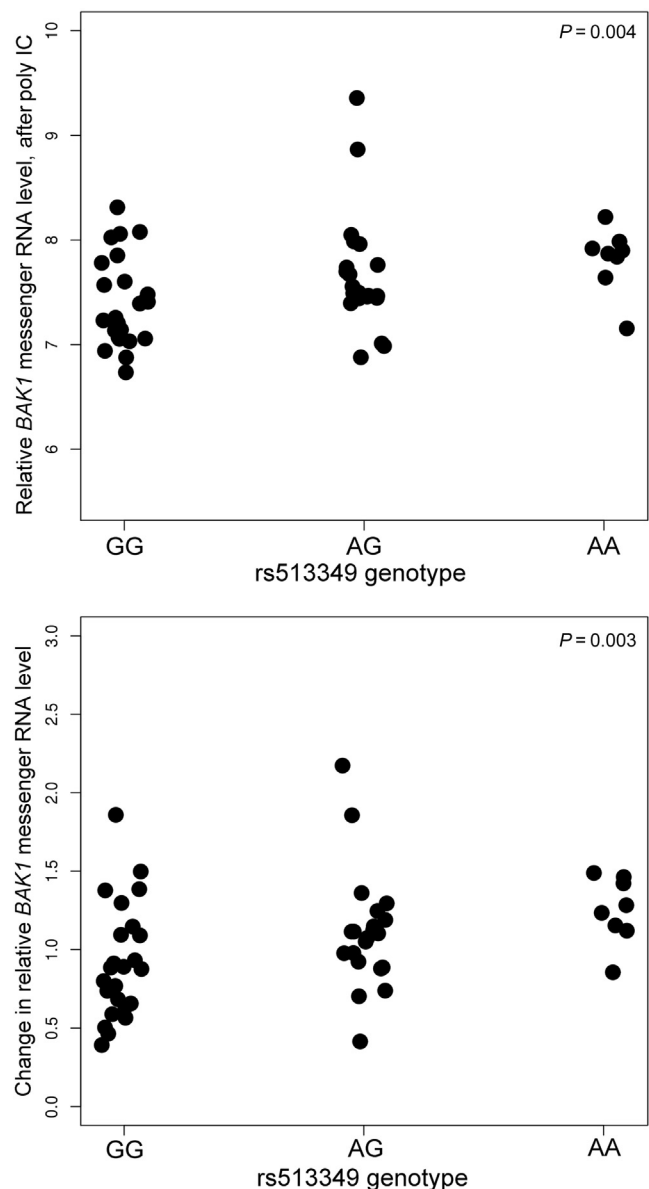


**Figure 2.** Relative *BAK1* expression versus single nucleotide polymorphism rs513349 in African American primary renal proximal tubule cell lines. Data expressed as mean  $\pm$  SD. (a) Post-polyinosinic-polycytidylic acid (poly IC) *BAK1* mRNA level versus rs513349 genotype. (b) Change in *BAK1* mRNA level (difference between post- and pre-poly IC versus rs513349 genotype). *P* values adjusted for African ancestry proportion.

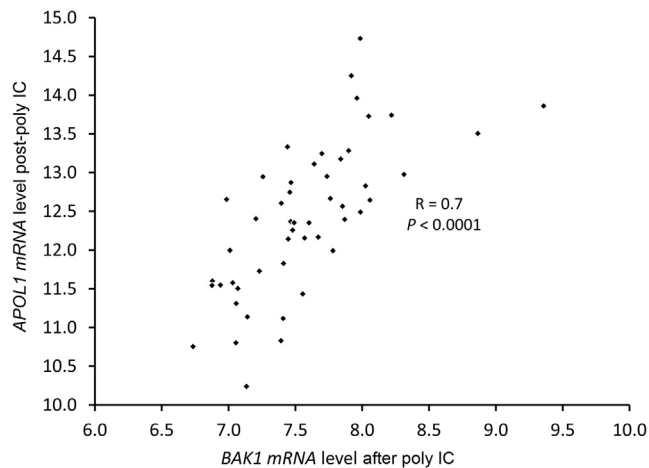


**Figure 3.** Relative *APOL1* versus *BAK1* mRNA expression levels in African American primary renal proximal tubule cells after polyinosinic-polycytidylic acid (poly IC). Linear regression was fitted between relative *APOL1* and *BAK1* mRNA expression levels.

### Mdivi-1 Restores Mitochondrial Membrane Potential in HEK293 Cells Overexpressing *APOL1* G1 and G2

Dox-induced *APOL1* G1 and G2 overexpression in HEK 293 Tet-on *APOL1* cells significantly reduced the relative mitochondrial membrane potential, defined as the fluorescence signal ratio of TMRE/MitoTracker Green. The relative mitochondrial membrane potential was partially restored in these cells after exposure to Mdivi-1 (Supplementary Figure S10). In contrast, Dox-induced overexpression in *APOL1* G0 and EV cells (and subsequent exposure to Mdivi-1) did not affect the relative mitochondrial membrane potential. Mdivi-1 did not alter relative mitochondrial membrane potential in the absence of mitochondrial depolarization. Results suggest that Mdivi-1 preserves mitochondrial architecture, resulting in improved mitochondrial membrane potential.

### Mdivi-1 Restores Viability of HEK293 Cells Overexpressing *APOL1* G1 and G2

To provide proof of concept that mitochondrial fusion/fission activity can be targeted in the treatment of *APOL1*-nephropathy, cell viability was assessed for HEK293 Tet-on *APOL1* G0, G1 and G2 cell lines at baseline, after Dox induction, and after Mdivi-1 rescue post-Dox induction. HEK293 Tet-on G0 cell (reference cells) viability was not altered after *APOL1* overexpression or treatment with Mdivi-1. For HEK293 Tet-on G1 and G2 cells, Dox-induced overexpression of both KRVs significantly reduced cell viability and Mdivi-1 restored cell viability, particularly at higher concentrations (Figure 6). Dose-response curves demonstrate increased viability of G1 and G2 cells with higher Mdivi-1 concentrations (Figure 6). In contrast to

Mdivi-1, the mitochondrial rescuer MitoQ did not alter the viability of cells induced by *APOL1* G1 and G2 variants (Supplementary Figure S11).

## DISCUSSION

*APOL1* KRVs induce mitochondrial dysfunction<sup>16,17</sup> and the present results support specific effects on mitochondrial dynamics that can be reversed with inhibitors of mitochondrial fission such as Mdivi-1. Global gene expression profiles were performed in primary renal PTC lines from African American individuals before and after poly IC to mimic innate immune system activation.<sup>21</sup> *APOL1* KRVs were not *cis* eQTLs for *APOL1* or adjacent genes, nor did they contribute to differences in global transcript expression attributed to poly IC. Relationships between other SNPs and *APOL1* expression were delineated using Illumina Multi-Ethnic Genotyping Arrays chip-based genome-wide genotyping. SNP rs513349 was among the top *trans* eQTLs for *APOL1* expression. This SNP was also a *cis* eQTL for the adjacent *BAK1* gene based on *cis* eQTL analyses in multiple human cells and tissues in the Genotype-Tissue Expression (GTEx) Project (*in silico* data retrieved December 19, 2019, from <https://www.gtexportal.org/>). *BAK1* and *APOL1* were co-expressed in primary renal PTCs after exposure to low concentrations of poly IC ( $R = 0.7$ ,  $P < 0.0001$ ) indicating that rs513349 acts as a *trans* eQTL for *APOL1* via regulation of *BAK1* expression on activation of the TLR3 pathway. As podocytes are critical cells in *APOL1*-nephropathy, *BAK1* was subsequently knocked out in a human podocyte cell line.<sup>30</sup> *APOL1* protein was markedly reduced in *BAK1* knockout cells, confirming the pivotal role of *BAK1* in *APOL1* expression. *BAK1* knockout did not inhibit *APOL1* messenger RNA levels when poly IC was absent; however, it did inhibit *APOL1* mRNA upregulation after poly IC treatment. This supports the initial eQTL analysis results. The phenomenon appears similar to that of a BCL2 family member, *BOK* (BCL2-related ovarian killer), the 3' untranslated region of which was modified by the presence of TRIM28. As a result, there was a lack of concordance between protein and transcript levels<sup>31</sup> and suggests that unstable mRNA may not generate proportional protein levels. The relationship between *BAK1* protein and the *APOL1* regulatory region (enhancer, promoter, and 3' untranslated region) requires further investigation. It would be ideal if *BAK1* could be knocked out in primary tubule cells with different *APOL1* genotypes. However, primary tubule cells can proliferate for only approximately 10 to 15 biological passages, typically within 3 weeks. This is approximately the time needed



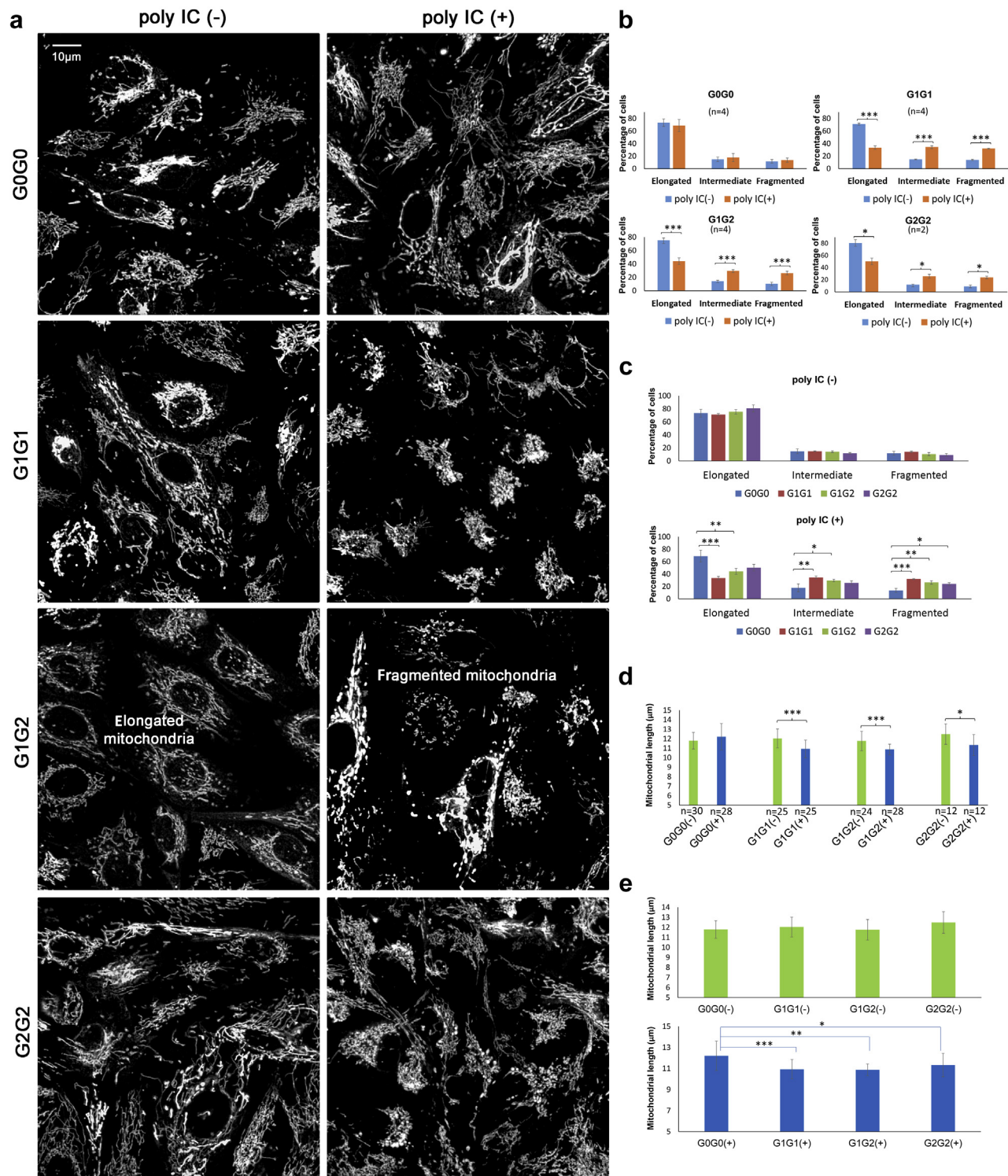


**Figure 4.** Mitochondrial morphology in live primary proximal tubule cell lines (PTCs) from African American individuals with different *APOL1* genotypes cultured in growth media without (–) and with (+) polyinosinic-polycytidylic acid (poly IC). Primary PTC lines were from 7 African American individuals (2 homozygous for *APOL1* G0, 2 homozygous for G1, 2 for compound G1/G2), and 1 homozygous for G2. Cells were grown without (–) or with (+) 2.5 μg/ml poly IC for 16 hours in full Dulbecco’s modified Eagle’s medium. Cells were subsequently incubated for 30 minutes with a final concentration of 50 nM MitoTracker Red (Invitrogen). (a) Representative images reveal that renal PTCs from the G0 homozygotes had similar mitochondrial morphology when incubated with (+) or without (–) poly IC. However, primary PTCs from G1 and G2 homozygotes and G1/G2 compound heterozygotes displayed more fragmented mitochondria when incubated with (+) poly IC than those without (–) poly IC. Each representative image was a compression of a series of z-stack scans, clearly capturing mitochondrial morphology. Binary images displayed with enhanced local contrast (CLAHE) via Fiji scoring by Mitochondrial Network Analysis. (b) Paired comparisons showing that the percentage of cells with mitochondrial elongation significantly decreased and the percentage of cells with mitochondria (continued)



for cells to go through the selection stage for CRISPR knockout. Hence, we were unable to perform experiments after knockout cells were created. This is a limitation of using primary cell lines.

BAK1 is a nuclear-encoded mitochondrial outer membrane protein.<sup>32</sup> APOL1 is also present in mitochondria and its G1 and G2 KRVs can induce mitochondrial dysfunction.<sup>16,17</sup> Although APOL1 KRVs induce cell death by mitochondrial translocation and opening of the mitochondrial permeability transition pore on the inner membrane,<sup>18</sup> other pathways may exist. APOL1 is co-expressed with the mitochondrial outer membrane protein BAK1, involved in mitochondrial dynamics via stabilization of phospho dynamin-related protein 1 (pDRP1) on the mitochondrial outer membrane.<sup>33</sup> Bax/Bak-dependent release of DDP/TIMM8a protein in the mitochondrial intermembrane space promotes DRP1-mediated mitochondrial fission and mitoptosis by redistributing pDRP to the mitochondrial outer membrane and inducing mitochondrial fission.<sup>34</sup>

The link between APOL1 and BAK1 in mitochondria led us to assess whether mitochondrial dynamics could compromise mitochondrial function induced by increased expression of APOL1 KRVs. Based on known effects of BAK1, we considered whether APOL1 KRVs altered mitochondrial morphology during fusion/fission. We found that mitochondria from human primary renal PTCs with 2 APOL1 KRVs were more likely to fragment after exposure to low concentrations of poly IC than those without KRVs (homozygous G0). The poly IC concentration for induction of APOL1 (2.5 µg/ml for 16 hours) was intentionally lower than

previously reported<sup>21</sup>; nonetheless, increases in APOL1 and TLR3 expression were similar to those with poly IC concentrations 5.0 or 10.0 µg/ml and cell viability was less impacted by the 2.5 µg/ml concentration (data not shown). Affymetrix HTA 2.0 array-based pathway analysis confirmed marked activation of the innate immune system with 2.5 µg/ml concentrations of poly IC (Supplementary Tables S1 and S2B). Fluorescence confocal microscopy performed on primary renal PTCs verified the mitochondrial morphology seen by transmission electron microscopy (data not shown) and confirmed increased mitochondrial fragmentation in cells with APOL1 KRVs after poly IC.

To determine whether enhanced mitochondrial fragmentation was a consequence of general innate immune system activation from poly IC or related to increased expression of APOL1 KRVs, HEK293 Tet-on APOL1 EV, G0, G1, and G2 cell lines conditionally overexpressing different APOL1 genotypes were examined. These were critical experiments because HEK293 cells lack innate immune system activation through the TLR3 pathway.<sup>26</sup> TLR3 mRNA was measured in HEK293 Tet-on EV, G0, G1, and G2 cells with and without poly IC, and expression was virtually undetectable (data not shown). Overexpression of APOL1 G1 and G2 in HEK293 cells promoted mitochondrial fragmentation (potentially via fission) based on confocal microscopy and supported by immunoblotting and immunofluorescence. This could relate to G1- and G2-mediated increases in active DRP1 (p-DRP1 at Ser 616). In contrast, overexpression of G0 reduced p-DRP1 (Ser616) levels in mitochondria, resulting in diminished fission and elongated mitochondria.

**Figure 4.** (continued) fragmentation significantly increased in primary renal PTCs with (+) poly IC than without (–) poly IC in subjects homozygous for G1, homozygous for G2, and compound G1/G2 heterozygotes. The percentage of cells with mitochondrial elongation and fragmentation did not differ in primary PTCs homozygous for G0. For each primary PTC line, 2 independent experiments were performed to image mitochondrial networks with or without poly IC. Primary PTCs from 2 African American individuals (1 woman and 1 man of comparable age) were selected for homozygous G0, homozygous G1, and compound G1/G2 genotypes. Only 1 homozygous G2 (female) had available primary PTCs. (Note: *n* refers to number of independent cell culture experiments; \**P* < 0.05, \*\* *P* < 0.01, \*\*\**P* < 0.001 throughout Figure 4; no statistical significance was found in any other paired comparison.) (c) Paired comparisons showing that the percentage of cells with mitochondrial elongation was significantly lower, and the percentage of cells with mitochondrial fragmentation significantly higher, in primary renal PTCs from G1 homozygotes and G1/G2 compound heterozygotes versus G0 homozygotes with poly IC in growth media. The effect in G2 homozygotes may have been limited by statistical power (1 individual, 2 independent experiments). The percentage of cells with mitochondrial elongation and fragmentation did not differ in primary PTCs of different APOL1 genotypes without poly IC. (d) Paired comparisons showing that mitochondrial length significantly decreased in primary renal PTCs with (+) poly IC versus without (–) poly IC in primary PTCs homozygous for G1, homozygous for G2 and compound G1/G2 heterozygotes; however, mitochondrial length did not differ in homozygous G0 primary PTCs with (+) or without (–) poly IC. *n* refers to the total number of images captured for Mitochondrial Network Analysis. At least 6 z-stack images were taken for each independent cell culture experiment. For cells of each PTC line, 2 independent experiments were performed for imaging mitochondrial networks with or without poly IC. Primary PTCs from 2 different African American individuals were selected for G0 homozygotes, G1 homozygotes, and compound G1/G2 heterozygotes; no significant difference in mitochondrial morphology (mitochondrial length defined as rods/network branches in µm) was observed between the 2 individuals of the same APOL1 genotype with or without poly IC. Only 1 G2 homozygote had available primary PTCs. (e) Mitochondrial length was comparable across primary PTCs with different APOL1 genotypes without poly IC. However, when cells were incubated with low-dose poly IC (2.5 µg/ml) for 16 hours, those possessing 2 APOL1 KRVs (homozygous G1, homozygous G2, and G1/G2 compound heterozygotes) appeared to have decreased mitochondrial length (more fragmented mitochondria were present).

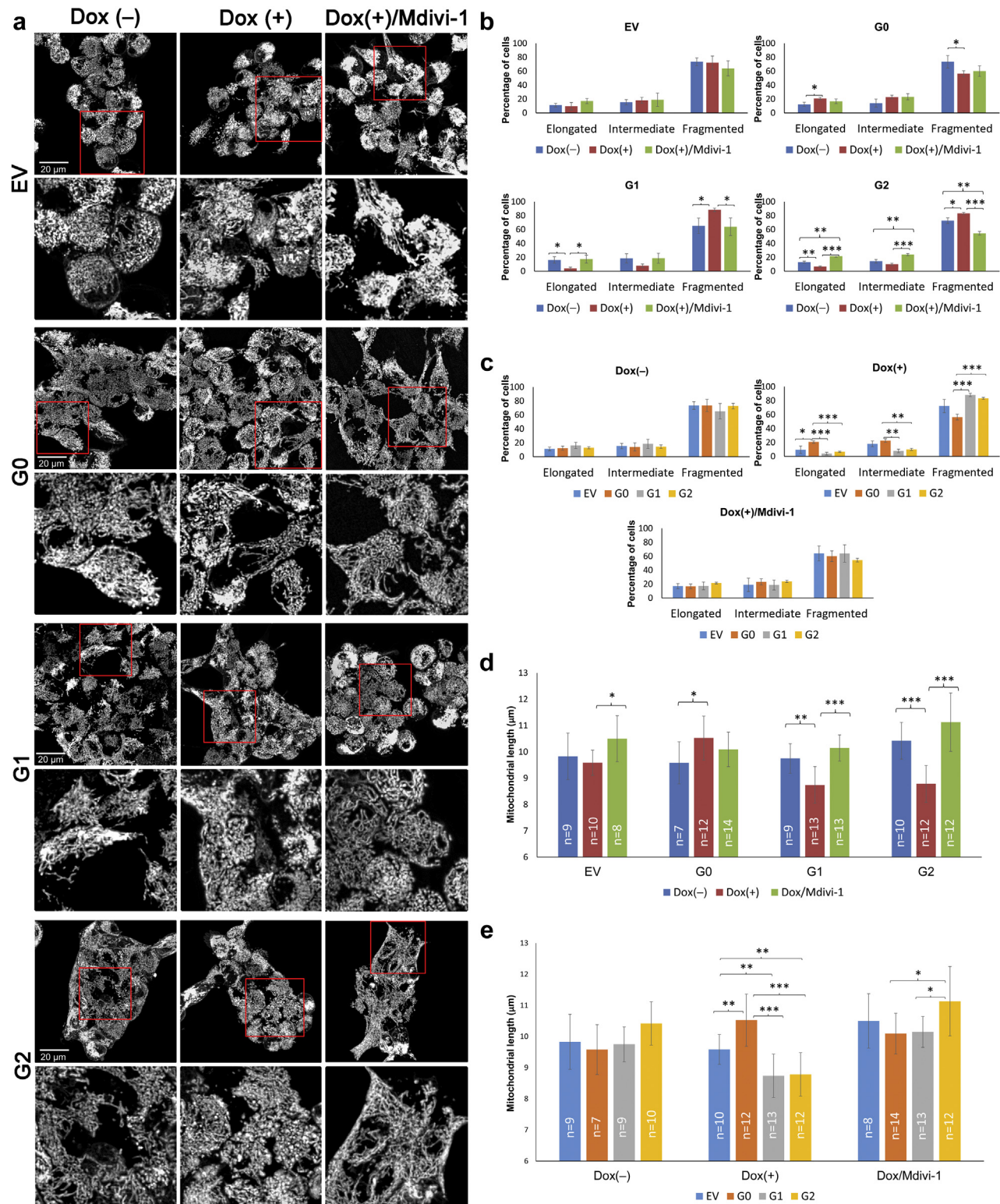


**Figure 5.** Confocal microscopy revealing altered mitochondrial morphology in HEK293 Tet-on *APOL1* cell lines in response to doxycycline (Dox) and Mdivi-1. HEK293 Tet-on empty vector (EV), G0, G1, or G2 cells were grown without (–) Dox and without Mdivi-1, with Dox (+) only, and with (+) Dox/Mdivi-1 for 16 hours in full Dulbecco’s modified Eagle’s medium. The final Dox concentrations were 10, 10, 5, 10 ng/ml for EV, G0, G1, and G2 cells, respectively; these conditions maintained cell viability and produced comparable *APOL1* overexpression levels in G0, G1, and G2 cells. In Dox (+) / Mdivi-1(+) cells, the final concentration for Mdivi-1 was 50  $\mu$ M. Cells were subsequently incubated for 30 minutes with a final concentration of 50 nM MitoTracker Red (Invitrogen). (a) HEK293 G0 cells displayed more elongated mitochondria when exposed to Dox. In contrast, HEK293 EV cells did not change markedly in response to Dox or Mdivi-1. Dox-induced *APOL1* G1 and G2 overexpression produced more fragmented mitochondria than without Dox. Addition of Mdivi-1 largely restored mitochondria to the tubular and elongated morphology in G1 and G2 cells with Dox induction. The red square was the imaged region for each cell type, detailed under the (continued)

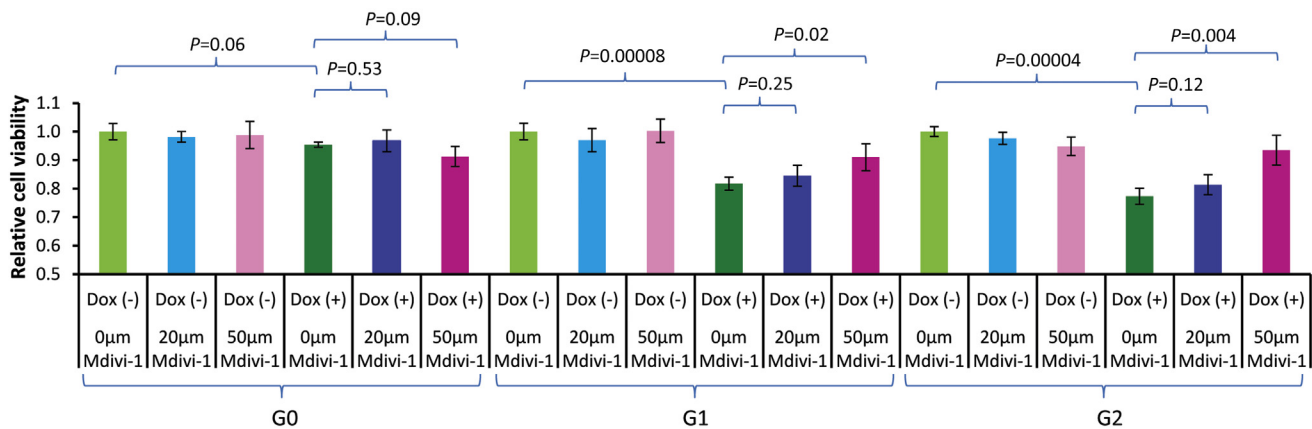


**Figure 6.** Cell viability in HEK293 Tet-on cells overexpressing *APOL1* G0, G1, and G2 when treated with Mdivi-1. HEK293 Tet-on G0, G1, or G2 cells were grown without (–) doxycycline (Dox) and with (+) 10 ng/ml Dox for 24 hours. The lactate dehydrogenase assay was used to assess cell viability. Final concentrations of Mdivi-1 (0, 20 μM, and 50 μM) were applied to HEK293 G0, G1, and G2 cells in Dox (–) and Dox (+) conditions ( $n = 4$  in each experiment). Dox induction did not affect cell viability in HEK293 Tet-on G0 cells; G1 and G2 cells had reduced viability after 24-hour Dox induction ( $P = 0.00008$  and  $0.00004$ , respectively). Mdivi-1 did not affect cell viability in HEK293 Tet-on G0, G1, and G2 cells without Dox induction. Mdivi-1 did not alter cell viability in G0 cells with or without Dox-induced *APOL1* overexpression. Mdivi-1 (50 μM) restored cell viability in Dox-induced G1 and G2 cells ( $P = 0.02$  and  $0.004$ , respectively); a dose-dependent pattern was seen. Note: Cells with (–)/(+) refer to without or with Dox induction, respectively.

Inhibition of mitochondrial fission by the DRP1 inhibitor Mdivi-1<sup>29</sup> appeared to preserve mitochondrial morphology. Mdivi-1 led to fewer fragmented mitochondria. Restoration of cell viability in HEK293 cells overexpressing G1 and G2 cells via Mdivi-1 provides additional evidence that altered mitochondrial dynamics play a role in the compromised mitochondrial function. In addition, Mdivi-1 restored cell viability in

HEK293 G1 and G2 cells in dose-dependent fashion (Figure 6). As such, the mitochondrial fusion/fission pathway may be a therapeutic target for reversing cellular dysfunction induced by *APOL1* KRVs. In contrast, the mitochondrial antioxidant MitoQ, a source of coenzyme Q, did not have this effect.

The mitochondrial dynamics pathway in HEK293 Tet-on cells was assessed via immunoblotting and

**Figure 5.** (continued) original image. Each image was representative of 18 scanned images from 3 independent experiments (binary images with enhanced local contrast [CLAHE] via Fiji scoring by Mitochondrial Network Analysis). (b) Comparison of mitochondrial morphology by *APOL1* induction and additional Mdivi-1 treatment in HEK293 Tet-on cells of different *APOL1* genotypes. Paired comparisons via 3 independent cell culture experiments showing that the percentage of cells with mitochondrial elongation significantly decreased and the percentage of cells with mitochondrial fragmentation significantly increased in HEK293 G1 and G2 cells with (+) Dox compared with those without (–) Dox. Mdivi-1 largely restored the mitochondrial pattern seen after Dox-induced *APOL1* overexpression in G1 and G2 cells. For HEK293 G0 cells, Dox-induced overexpression of *APOL1* increased the percentage of elongated cells and decreased the percentage of fragmented cells compared with those without (–) Dox, suggesting G0 may be beneficial to mitochondrial morphology; however, Mdivi-1 did not further alter the mitochondrial morphology of these cells. HEK293 EV Tet-on cells did not display changes in mitochondrial elongation or fragmentation with Dox or Mdivi-1. (Note: \* $P < 0.05$ , \*\* $P < 0.01$ , \*\*\* $P < 0.001$  throughout Figure 5; no statistical significance found in any other paired comparison.) (c) Comparison of mitochondrial morphology by *APOL1* genotype in HEK293 Tet-on cells without Dox induction, with Dox induction, and after Mdivi-1. Paired comparisons via 3 independent cell culture experiments showing that the percentage of cells with elongated and fragmented mitochondria were comparable among HEK293 cells of different *APOL1* genotypes when Dox was absent. When *APOL1* expression was induced by Dox, the percentage of cells with elongated mitochondria was significantly lower and the percentage of cells with fragmented mitochondria was significantly higher in HEK293 G1 and G2 cells than G0 cells. Mitochondrial morphology did not differ in Dox-induced HEK293 EV, G0, G1, and G2 cells with addition of Mdivi-1. (d) Mitochondrial length (rods/network branches) by *APOL1* genotype in HEK293 Tet-on cells without Dox induction, with Dox induction, and after Mdivi-1. Mitochondrial length, defined by rods/network branches, was estimated using Fiji integrated with the plug-in macro toolset Mitochondrial Network Analysis. Mitochondrial length did not differ in HEK293 Tet-on EV cells regardless of Dox induction or Mdivi-1 addition. Mitochondrial length increased in HEK293 Tet-on G0 cells when induced by Dox; however, it was not further affected by the addition of Mdivi-1. Mitochondrial length decreased significantly in HEK293 Tet-on G1 and G2 cells when induced by Dox, indicating enhanced mitochondrial fragmentation by overexpression of G1 and G2 variants. Reduced mitochondrial length was restored after addition of Mdivi-1. (Note:  $n$  refers to number of images.) (e) Mitochondrial branch length by Dox induction and additional Mdivi-1 treatment in HEK293 Tet-on cells of different *APOL1* genotypes. Mitochondrial length was largely comparable for HEK293 Tet-on cells of different *APOL1* genotypes without Dox. With Dox-induced *APOL1* overexpression, G0 cells appeared to have significantly higher mitochondria length than G1 and G2, indicating *APOL1* G0 promoted mitochondrial elongation, whereas G1 and G2 variants enhanced mitochondrial fragmentation. Mitochondrial length was relatively comparable for Dox-induced EV, G0, G1, and G2 cells when Mdivi-1 was added, slightly longer mitochondria were seen in G2 cells.



fluorescence microscopy after 16-hour and 24-hour Dox induction. The 16-hour Dox induction minimized the impact of cell viability (Supplementary Figure S12) when examining the mitochondrial morphology and function, whereas the 24-hour Dox induction maximized the effect of *APOL1* G1 and G2 variants when most cells remained viable and cell viability could be restored. Both Dox-induction conditions produced comparable levels of *APOL1* overexpression (Supplementary Figures S7 and S13).

The expected reduction in relative mitochondrial membrane potential for G1 and G2 cells was observed, reproducing the pattern in our prior report with higher concentration Dox induction and shorter exposure time.<sup>16</sup> Mdivi-1 significantly increased the relative membrane potential in *APOL1* G1 and G2 cells after low-concentration Dox induction. Mdivi-1 appeared to improve cell viability by preventing mitochondrial fragmentation and preserving membrane potentials in G1 and G2 cells, but it did not increase the membrane potential in Dox-induced G0 cells. This demonstrates specific efficacy of Mdivi-1 in mitochondrial dysfunction related to G1 and G2. Results were supported by morphological studies; however, it is unlikely that mitochondrial fission is the sole pathway compromising mitochondrial function because Mdivi-1 largely restored mitochondrial length in Dox-induced HEK293 G1 and G2 cells (Figure 5d and e) without fully restoring the mitochondrial membrane potential (Supplementary Figure S10). Results do not exclude additional effects of *APOL1* on mitochondrial dynamic pathways beyond pDRP1, such as activated mitochondrial permeability transition.<sup>18</sup> Bordt *et al.*<sup>35</sup> questioned the specificity of Mdivi-1 as a mitochondrial fission inhibitor in ischemia-reperfusion injury experiments. However, Manczak *et al.*<sup>36</sup> confirmed that Mdivi-1 is a DRP-1 inhibitor and directly reduces

mitochondrial fission. MitoQ was developed as a mitochondrial-targeted antioxidant for diseases associated with oxidative stress. MitoQ reportedly blocks the generation of reactive oxygen species.<sup>37</sup> Therefore, we assessed MitoQ in parallel with Mdivi-1, in rescue experiments performed in HEK293 Tet-on cells overexpressing *APOL1* G0, G1, and G2. As shown in Figure 6, Mdivi-1 significantly restored cell viability, whereas MitoQ did not (Supplementary Figure S11). This indicates that mitochondrial fragmentation/fission is the likeliest pathway whereby *APOL1* G1 and G2 variants induce mitochondrial dysfunction, whereas targeting reactive oxygen species may be less specific. It has been reported that mutations at Ser616 in DRP1 (phosphorylation site) or inhibiting DRP1 activity blocks mitochondrial permeability transition pore opening.<sup>38</sup> This suggests that mitochondrial fission is an event upstream from mitochondrial permeability transition pore opening.

Removal of damaged mitochondria through autophagy or mitophagy, a process selectively removing damaged or excessive mitochondria, is critical to maintain cellular function,<sup>39</sup> especially in podocytes<sup>40</sup> and PTCs.<sup>41</sup> Permanent loss of function or death of podocytes can have irreversible consequences on kidney function. Fragmented mitochondria are eliminated by autophagy when a threshold of cellular damage develops. Fission may segregate the most severely damaged mitochondria to preserve the health of the mitochondrial network.<sup>42</sup> If G1 and G2 variant-induced mitochondrial damage/fragmentation cannot be compensated by appropriate mitophagy, possibly due to defective intracellular trafficking as proposed,<sup>5,43</sup> cell death machinery may be activated.<sup>32</sup>

Figure 7 displays a diagram with potential mechanisms of *APOL1* KRV-induced mitochondrial

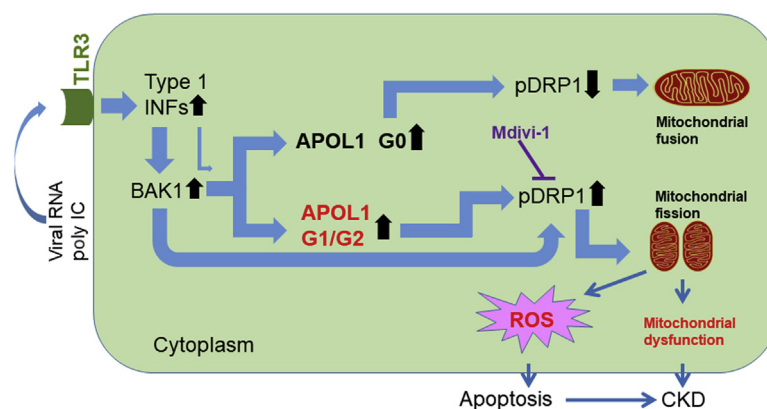


**Figure 7.** Diagram showing potential mechanisms of *APOL1* kidney-risk variant-induced mitochondrial dysfunction. CKD, chronic kidney disease; INF, interferon; pDRP1, phospho dynamin-related protein 1; poly IC, polyinosinic-polycytidylic acid; ROS, reactive oxygen species; TLR3, Toll-like receptor 3.



dysfunction. In response to environmental stressors, such as viral infection, *APOL1* is upregulated through the TLR3 pathway via increased type 1 interferons.<sup>21</sup> However, *BAK1* is a more robust inducer of *APOL1* than interferons; *BAK1* knockout markedly reduced *APOL1* expression. *BAK1* promotes mitochondrial outer membrane permeabilization.<sup>44</sup> During apoptosis, Bax/Bak-dependent release of DDP/TIMM8a protein in the mitochondrial intermembrane space promotes DRP1-mediated mitochondrial fission and mitoptosis by redistributing pDRP to the mitochondrial outer membrane and inducing mitochondrial fission.<sup>34</sup> As a result of innate immunity, type 1 interferons increase *BAK1* expression for mitoptosis and apoptosis.<sup>45</sup> A limitation of the study is the lack of kidney sections from patients with chronic kidney disease. As such, we were unable to display *BAK1* distribution in the context of kidney disease. Increased levels of *APOL1* G0 protein appear to counter effects of *BAK1*; G0 preserves mitochondrial function by inhibiting DRP1 expression. This results in mitochondrial fusion. As *APOL1* upregulation by *BAK1* is independent of *APOL1* genotype, increased levels of *APOL1* G1 and G2 protein may reduce inhibition to DRP1 expression. These promote mitochondrial fission. Fission was reversed by the DRP1 inhibitor Mdivi-1. In addition to the deleterious effect of the KRVs on mitochondrial integrity, the “beneficial” effects of G0 upregulation on mild inhibition of p-DRP1 (Supplementary Figure S8) and decreased endoplasmic reticulum stress<sup>16</sup> were absent for G1 or G2 KRVs. Mitochondrial membrane potentials decrease during mitochondrial fission. This effect may be independent from the mechanism proposed by Shah *et al.*,<sup>18</sup> where the mitochondrial permeability transition pore opened when binding G1 or G2 variants with decreased mitochondrial membrane potential. This might explain why Mdivi-1 did not fully restore cell viability and mitochondrial membrane potential when *APOL1* G1 and G2 were induced in HEK293 Tet-on cells. Although *BAK1* clearly upregulates *APOL1*, details of this pathway require further investigation.

This series of experiments used unique human primary renal PTC lines from African American individuals to explore potential effects of *APOL1* on human kidney cells, with replication in HEK293 Tet-on *APOL1* cells. Results in human primary renal PTC cells with different *APOL1* genotypes implicated altered mitochondrial dynamics on risk for *APOL1*-nephropathy. Cell viability and mitochondrial dynamics were improved in cells with *APOL1* KRVs after exposure to Mdivi-1, an inhibitor of DRP1 and mitochondrial fission. Future studies involving mitochondrial

dynamics and mutations could further inform the field regarding *APOL1* KRV effects on nephropathy. This may lead to novel therapies for *APOL1*-associated disorders.

## DISCLOSURE

Wake Forest University Health Sciences and BIF have rights to an issued U.S. patent related to *APOL1* genetic testing. BIF is a consultant for AstraZeneca and RenalytixAI Pharmaceuticals. All the other authors declared no competing interests.

## ACKNOWLEDGMENTS

We thank Dr. Martin R. Pollak for sharing *APOL1* vectors. This work was supported by National Institutes of Health (NIH) grants R01 DK070941 (BIF), R01 DK084149 (BIF), and R01 MD009055 (JD, BIF), and P30 CA012197 (Wake Forest Comprehensive Cancer Center). The NIH GEO database access for this project is GSE119958.

## AUTHOR CONTRIBUTIONS

LM, BIF, and AJAM designed the study; LM and BIF drafted and revised the paper; JSP provided in-depth revision; LM, JAS, YAC, MSB, DC, ALC, and PJH performed the experiments; HCA, LM, JWC, CDL, and JD analyzed the data; MM and AKH recruited subjects and revised the paper; SP provided microscopy assistance and revised the paper; GAH and LDM provided global gene expression technical expertise and reviewed the manuscript; and MAS provided human immortalized podocyte and proximal tubular cell lines, helped establish cell culture conditions, and reviewed the paper. All authors approved the final version of the manuscript.

## SUPPLEMENTARY MATERIAL

[Supplementary File \(PDF\)](#)

### Supplementary Methods.

**Figure S1.** Presence of *BAK1* protein in human renal proximal tubule cells (PTCs).

**Figure S2.** Presence of *BAK1* protein in immortalized podocytes.

**Figure S3.** Presence of *BAK1* on nondiseased human kidney cryosections.

**Figure S4.** *APOL1* messenger RNA level responses to the presence of poly IC and *BAK1* by RT-PCR.

**Figure S5.** *APOL1* protein level responses to the presence of *BAK1* by immunoblotting.

**Figure S6.** *APOL1* protein level responses to the presence of *BAK1* by immunofluorescence.

**Figure S7.** Comparison of *APOL1* gene expression in HEK293 Tet-on cells.

**Figure S8.** Mitochondrial fission marker DRP1 increased in Dox-induced HEK293 Tet-on G1 and G2 cell lines.

**Figure S9.** Phospho-DRP1 at Ser 616 (pDRP1) responds to APOL1 overexpression and Mdivi-1 rescue.

**Figure S10.** Relative mitochondrial membrane potential was reduced in Dox-induced HEK293 Tet-on APOL1 G1 and G2 cells and rescued by Mdivi-1.

**Figure S11.** Cell viability in HEK293 Tet-on cells overexpressing APOL1 G0, G1, and G2 when treated with MitoQ.

**Figure S12.** Quantitative cell viability in HEK293 Tet-on EV, G0, G1, or G2 cells after 16-hour Dox induction.

**Figure S13.** Relative APOL1 expression levels were comparable in HEK293 Tet-on cells with Dox induction for 16 hours.

**Table S1.** Top 20 most differentially expressed pathways (1060 downregulated and 1212 upregulated) after poly IC in the 50 African American primary renal PTC lines using Cytoscape BiNGO.

**Table S2A.** Top canonical pathways detected based on the most downregulated genes by poly IC in 50 primary African American renal PTC lines using Ingenuity Pathway Analysis.

**Table S2B.** Top canonical pathways detected based on the most upregulated genes by poly IC in 50 primary African American renal PTC lines using Ingenuity Pathway Analysis.

## REFERENCES

- Genovese G, Friedman DJ, Ross MD, et al. Association of trypanolytic ApoL1 variants with kidney disease in African Americans. *Science*. 2010;329:841–845.
- Tzur S, Rosset S, Shemer R, et al. Missense mutations in the APOL1 gene are highly associated with end stage kidney disease risk previously attributed to the MYH9 gene. *Hum Genet*. 2010;128:345–350.
- Olabisi OA, Zhang J-Y, VerPlank L, et al. APOL1 kidney disease risk variants cause cytotoxicity by depleting cellular potassium and inducing stress-activated protein kinases. *Proc Natl Acad Sci U S A*. 2016;113:830–837.
- Fu Y, Zhu J, Richman A, et al. APOL1-G1 in nephrocytes induces hypertrophy and accelerates cell death. *J Am Soc Nephrol*. 2016;28:1106–1116.
- Kruzel-Davila E, Shemer R, Ofir A, et al. APOL1-mediated cell injury involves disruption of conserved trafficking processes. *J Am Soc Nephrol*. 2017;28:1117–1130.
- Bruggeman LA, O'Toole JF, Ross MD, et al. Plasma apolipoprotein L1 levels do not correlate with CKD. *J Am Soc Nephrol*. 2014;25:634–644.
- Weckerle A, Snipes JA, Cheng D, et al. Characterization of circulating APOL1 protein complexes in African Americans. *J Lipid Res*. 2016;57:120–130.
- Kozlitina J, Zhou H, Brown PN, et al. Plasma levels of risk-variant APOL1 do not associate with renal disease in a population-based cohort. *J Am Soc Nephrol*. 2016;27:3204–3219.
- Madhavan SM, O'Toole JF, Konieczkowski M, et al. APOL1 localization in normal kidney and nondiabetic kidney disease. *J Am Soc Nephrol*. 2011;22:2119–2128.
- Ma L, Shelness GS, Snipes JA, et al. Localization of APOL1 protein and mRNA in the human kidney: nondiseased tissue, primary cells, and immortalized cell lines. *J Am Soc Nephrol*. 2015;26:339–348.
- Freedman BI, Pastan SO, Israni AK, et al. APOL1 genotype and kidney transplantation outcomes from deceased African American donors. *Transplantation*. 2016;100:194–202.
- Freedman BI, Julian BA, Pastan SO, et al. Apolipoprotein L1 gene variants in deceased organ donors are associated with renal allograft failure. *Am J Transplant*. 2015;15:1615–1622.
- Reeves-Daniel AM, DePalma JA, Bleyer AJ, et al. The APOL1 gene and allograft survival after kidney transplantation. *Am J Transplant*. 2011;11:1025–1030.
- Lee BT, Kumar V, Williams TA, et al. The APOL1 genotype of African American kidney transplant recipients does not impact 5-year allograft survival. *Am J Transplant*. 2012;12:1924–1928.
- Beckerman P, Bi-Karchin J, Park ASD, et al. Transgenic expression of human APOL1 risk variants in podocytes induces kidney disease in mice. *Nat Med*. 2017;23:429–438.
- Ma L, Chou JW, Snipes JA, et al. APOL1 Renal-Risk Variants Induce Mitochondrial Dysfunction. *J Am Soc Nephrol*. 2017;28:1093–1105.
- Granado D, Müller D, Krausel V, et al. Intracellular APOL1 risk variants cause cytotoxicity accompanied by energy depletion. *J Am Soc Nephrol*. 2017;28:3227–3238.
- Shah SS, Lannon H, Dias L, et al. APOL1 kidney risk variants induce cell death mitochondrial translocation and opening of the mitochondrial permeability transition pore. *J Am Soc Nephrol*. 2019;2355–2368.
- Galvan DL, Green NH, Danesh FR. The hallmarks of mitochondrial dysfunction in chronic kidney disease. *Kidney Int*. 2017;92:1051–1057.
- Freedman BI, Skorecki K. Gene-gene and gene-environment interactions in apolipoprotein L1 gene-associated nephropathy. *Clin J Am Soc Nephrol*. 2014;9:2006–2013.
- Nichols B, Jog P, Lee JH, et al. Innate immunity pathways regulate the nephropathy gene Apolipoprotein L1. *Kidney Int*. 2015;87:332–342.
- Cheng D, Weckerle A, Yu Y, et al. Biogenesis and cytotoxicity of APOL1 renal risk variant proteins in hepatocytes and hepatoma cells. *J Lipid Res*. 2015;56:1583–1593.
- Ma L, Murea M, Snipes JA, et al. An ACACB variant implicated in diabetic nephropathy associates with body mass index and gene expression in obese subjects. *PLoS One*. 2013;8:e56193.
- Valente AJ, Maddalena LA, Robb EL, et al. A simple ImageJ macro tool for analyzing mitochondrial network morphology in mammalian cell culture. *Acta Histochem*. 2017;119:315–326.
- Karbowski M, Norris KL, Cleland MM, et al. Role of Bax and Bak in mitochondrial morphogenesis. *Nature*. 2006;443:658–662.
- Sarkar SN, Smith HL, Rowe TM, et al. Double-stranded RNA signaling by Toll-like receptor 3 requires specific tyrosine

- residues in its cytoplasmic domain. *J Biol Chem.* 2002;278:4393–4396.
27. Cereghetti GM, Stangherlin A, de Brito OM, et al. Dephosphorylation by calcineurin regulates translocation of Drp1 to mitochondria. *Proc Natl Acad Sci U S A.* 2008;105:15803–15808.
  28. Kashatus JA, Nascimento A, Myers LJ, et al. Erk2 phosphorylation of Drp1 promotes mitochondrial fission and MAPK-driven tumor growth. *Mol Cell.* 2015;57:537–551.
  29. Kim H, Lee JY, Park KJ, et al. A mitochondrial division inhibitor, Mdivi-1, inhibits mitochondrial fragmentation and attenuates kainic acid-induced hippocampal cell death. *BMC Neurosci.* 2016;17:33.
  30. Saleem MA, O'Hare MJ, Reiser J, et al. A conditionally immortalized human podocyte cell line demonstrating nephrin and podocin expression. *J Am Soc Nephrol.* 2002;13:630–638.
  31. Fernandez-Marrero Y, Bachmann D, Lauber E, et al. Negative regulation of BOK expression by recruitment of TRIM28 to regulatory elements in its 3' untranslated region. *iScience.* 2018;9:461–474.
  32. Boland ML, Chourasia AH, Macleod KF. Mitochondrial dysfunction in cancer. *Front Oncol.* 2013;3:292.
  33. Wasiak S, Zunino R, McBride HM. Bax/Bak promote sumoylation of DRP1 and its stable association with mitochondria during apoptotic cell death. *J Cell Biol.* 2007;177:439–450.
  34. Arnoult D, Rismanchi N, Grodet A, et al. Bax/Bak-dependent release of DDP/TIMM8a promotes Drp1-mediated mitochondrial fission and mitoptosis during programmed cell death. *Curr Biol.* 2005;15:2112–2118.
  35. Bordt EA, Clerc P, Roelofs BA, et al. The putative Drp1 inhibitor mdivi-1 is a reversible mitochondrial complex I inhibitor that modulates reactive oxygen species. *Dev Cell.* 2017;40:583–594.e6.
  36. Manczak M, Kandimalla R, Yin X, et al. Mitochondrial division inhibitor 1 reduces dynamin-related protein 1 and mitochondrial fission activity. *Hum Mol Genet.* 2019;28:177–199.
  37. Lu C, Zhang D, Whiteman M, et al. Is antioxidant potential of the mitochondrial targeted ubiquinone derivative MitoQ conserved in cells lacking mtDNA? *Antioxid Redox Signal.* 2008;10:651–660.
  38. Xu S, Wang P, Zhang H, et al. CaMKII induces permeability transition through Drp1 phosphorylation during chronic  $\beta$ -AR stimulation. *Nat Commun.* 2016;7:13189.
  39. Um J-H, Yun J. Emerging role of mitophagy in human diseases and physiology. *BMB Rep.* 2017;50:299–307.
  40. Hartleben B, Gödel M, Meyer-Schwesinger C, et al. Autophagy influences glomerular disease susceptibility and maintains podocyte homeostasis in aging mice. *J. Clin. Invest.* 2010;120:1084–1096.
  41. Tang C, He L, Liu J, et al. Mitophagy: basic mechanism and potential role in kidney diseases. *Kidney Dis.* 2015;1:71–79.
  42. Youle RJ, van der Bliek AM. Mitochondrial fission, fusion, and stress. *Science.* 2012;337:1062–1065.
  43. Madhavan SM, O'Toole JF, Konieczkowski M, et al. APOL1 variants change C-terminal conformational dynamics and binding to SNARE protein VAMP8. *JCI Insight.* 2017;2(14).
  44. Peña-Blanco A, García-Sáez AJ. Bax, Bak and beyond—mitochondrial performance in apoptosis. *FEBS J.* 2018;285:416–431.
  45. Fraietta JA, Mueller YM, Yang G, et al. Type I interferon upregulates Bak and contributes to T cell loss during human immunodeficiency virus (HIV) infection. *PLoS Pathog.* 2013;9:e1003658.